APPLYING A MODIFIED AUSTENITE TRANSFORMATION MODEL INTO A THERMO-MECHANICAL MODEL OF HOT STAMPING

Amir Abdollahpoor[1*], Xiangjun Chen[3,4], Michael Pereira[2], Alireza Asgari[1], Namin Xiao[3], Bernard Rolfe[1]

[1] School of Engineering, Deakin University, Geelong, Australia
[2] Institute for Frontier Materials, Deakin University, Geelong, Australia
[3] Institute of Metal Research, Chinese Academy of Sciences, Shenyang, China
[4] State Key Laboratory of Advanced Design and Manufacturing for Vehicle Body, Hunan University, Changsha, China

ABSTRACT: Hot stamping is an innovative forming process for the production of vehicle body parts with complicated geometries and high strength. In this process, hot sheet metal is formed within a die and cooled down at the same time. The cooling rates are critical to the final microstructure and thus the final mechanical properties of the part in service (strength, ductility, energy absorption ability). Therefore, an accurate model that can predict the thermo-mechanical-metallurgical characteristics of the process is increasingly important. In this paper, a thermo-mechanical finite element model of hot stamping is created and a modified phase transformation model based on Scheil's additive principle has been applied. The comparison between the modeling and experiment shows that the modified phase transformation model coupled with the incubation time provides higher accuracy on the simulation of transformation kinetics history. In the stamping process, the effect of different die materials and increasing the die temperature to reduce the sheet cooling rate is analyzed in this paper. This work demonstrates the application of the combined thermo-mechanical-metallurgical model in hot stamping. Additionally, the results provide insights into the use of locally differentiated cooling rates, either via local die material changes or selective heating, to produce tailored mechanical properties in hot stamped components.

KEYWORDS: Hot stamping, Numerical modeling, Phase transformation

1 INTRODUCTION

In hot stamping of boron steels, sheet metal is heated in a furnace from room temperature with ferrite-pearlite microstructure up to approximately 930°C where full austenitization occurs [1]. Then, the forming process is done in a water-cooled die and must be finished in temperatures higher than the Martensite start (Ms) temperature. The next operation is to cool down the formed component in the die with rates higher than approximately 27°C/s to allow full martensite evolution in the microstructure. Phase transformation from austenite to full martensite increases tensile strength from 600 MPa up to 1500 MPa in the final product. On the other hand, the material properties at the high forming temperatures increase formability and reduce press forces, tool wear and springback.

The high tensile strengths achievable by hot stamping increase part integrity during crashes and this is beneficial, especially where the intrusion is not allowed due to the requirement to protect the occupant compartment. On the other hand, there is a need to profit from high ductility in crumple zones to absorb crash energy by consuming it in plastic work. The simultaneous need for both high strength and high ductility in some vehicle parts (e.g. B-Pillar) has encouraged engineers to find design solutions such as vehicle parts with tailored mechanical properties (Fig. 1). Different solutions have been investigated, but the most developed solution in hot stamped components is to locally differentiate the cooling rate in the die. Using this method, the cooling rate in the blank material is slowed down to lower than 27°C/s in the zone where high ductility is desired. This results in the evolution of daughter phases: ferrite, bainite and pearlite. There are two main solutions to achieve

* Corresponding author:
Deakin University, Locked Bag 20000, Geelong, VIC 3220.
Phone: 0061-415214139
Email: aabdolla@deakin.edu

different cooling rates in a single die. The first method is to heat the die partially to reduce the cooling rate and to cool the remaining sections of the die to increase cooling rate. The second method is to use different tool material with different heat conduction coefficients [2].

In this study, a thermo-mechanical-metallurgical finite element model of hot stamping will be used to investigate the effects of tool temperature and material on the cooling rates and consequent microstructural phases. A modified phase transformation model has been applied to improve the accuracy of the prediction of phase fractions in the final component.

Fig. 1 *A sample B-Pillar with tailored mechanical properties*

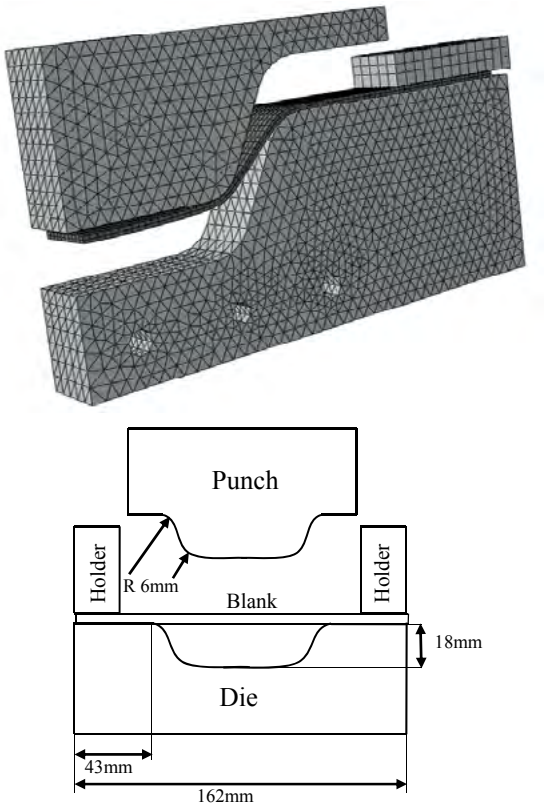

Fig. 2 *A hat-shaped sample in FEM model*

2 NUMERICAL SIMULATION

2.1 GENERAL ASPECTS

Hot stamping is a thermo-mechanical-metallurgical process. The forming and quenching processes of a simple hat-shaped component have been simultaneously modelled in FEM software ABAQUS Standard V6.12 (Fig. 2). The transfer process from the furnace to the die is ignored in the model. However, it is assumed that the temperature of the blank has been reduced from 930°C to 800°C due to cooling during the transfer process. A modified phase transformation model based on Scheil's additive principle has been applied to the thermo-mechanical model using an ABAQUS Subroutine to predict resultant steel phases in the final product. The punch, die and blank holder have been considered as deformable bodies that enables the study of heat transfer through them.

Symmetry boundary conditions have been applied to the blank and tool which allows just one quarter of the geometry to be modelled. The blank and blank-holder were modelled with 8-node brick elements, while tetrahedral elements are used to mesh the punch and the die. Further to the forming and quenching steps, extra steps were defined to establish contact between the tooling and blank prior to the main forming process and also to apply boundary conditions.

2.2 MATERIAL MODEL

Boron steel sheet (22MnB5) has been modelled with temperature dependant thermo-mechanical properties. Due to the wide range of working temperature in hot stamping, ignoring these dependencies will significantly reduce the precision of the results. Fig. 3 shows the stress-strain curves for boron steel 22MnB5 used in this study [3]. The flow curves at different temperatures at a strain rate $0.1s^{-1}$ were applied. The dependency of material flow data to strain rate is ignored in this study.

The properties of the blank, including Young's modulus (E), Poisson's ratio (ϑ), thermal conductivity (k) and specific heat capacity (C_P) were defined to include temperature dependency, and are shown in Table 1. The inelastic heat fraction parameter, which defines the heating associated with plastic work of the blank material, was set to the default value of 0.9. Also, the frictional heating has been considered in this model.

Four different tool materials have been considered in this study; AISI h11, Alumina, Macor® and Zirconia. Table 2 shows thermo-mechanical properties of these materials. Different properties of these materials will result in different cooling rates and microstructural phases. Due to the significantly smaller range of temperature occurring in tool, temperature independent properties have been used.

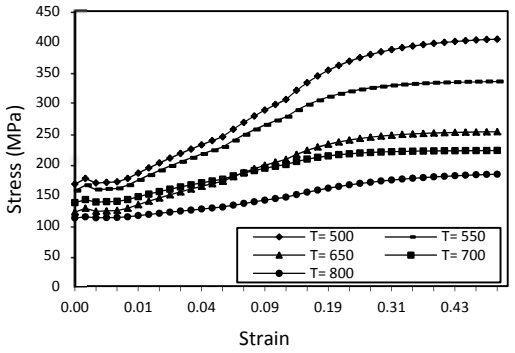

Fig. 3 *Stress-Strain curves for boron steel 22MnB5 for different temperatures in strain rate 0.1 s^{-1} [3]*

Table 1: *Thermomechanical properties as a function of temperature for boron steel 22MnB5 [5]*

Temperature (°C)	E (GPa)	ν	K (W/m°C)	C_p (J/kg°C)
20	212	0.284	30.7	444
100	207	0.286	31.1	487
200	199	0.289	30.0	520
300	193	0.293	27.5	544
400	166	0.298	21.7	561
500	158	0.303		573
600	150	0.310	23.6	581
700	142	0.317		586
800	134	0.325	25.6	590
900	126	0.334		596
1000	118	0.343	27.6	603

Table 2: *Thermomechanical properties of investigated tool materials used in this study [4]*

	AISI h11	Alumina	Macor	Zirconia
E (Gpa)	210	360	67	210
C (J/kg per K)	526	510	790	400
K (W/m per K)	42.2	19	1.46	2.5
ρ (kg/m^3)	7750	3850	2520	6040

2.3 CONTACT MODEL

Thermo-mechanical contact behaviour between the blank and tools surfaces have been considered in this model. The mechanical contact has been defined using Penalty friction formulation, with the friction coefficient as a function of temperature [6]. The thermal contact behaviour has been taken into account by defining contact heat transfer coefficient. It has been shown that this coefficient is in a direct relation with contact pressure [4]. The dependency of contact heat conductance to contact pressure has been shown in Table 3 for all tool materials investigated in this study. The punch-blank and die-blank contacts were defined using the "Node to Surface" discretization method.

2.4 TOOL TEMPERATURE

In conventional hot stamping processes, the tools are water-cooled to achieve fast blank cooling rates and therefore a 100% martensite volume fraction in the final part. There are a number of solutions to prevent full martensite transformation. The most common approach to produce hot stamped parts with tailored mechanical properties is to alter the cooling rates in a single die.

Table 3: *Contact Heat Conductance (nominal measures) in different contact pressures [4]*

Contact Pressure	Contact Heat Conductance $(W/m^2 per\ K)$			
	AISI h11	Alumina	Macor	Zirconia
5 MPa	3175	778	240	497
10 MPa	3300	1183	268	651
20 MPa	3975	1475	260	724
30 MPa	4150	1225	280	711
40 MPa	4025	1700	280	676

Several researchers have considered the effects of tool temperatures on the cooling rates. To achieve the high fractions of martensite, tool materials with higher conductivity are selected to accelerate the cooling. In the case of using the same tool material to slow down the cooling in the interest of achieving higher ductility, higher tool temperatures are needed in comparison with using tool materials with lower conductivity. It implies that using alternatives tool materials with lower conductivities and heat contact conductance reduces the amount of energy needed for tool heating. To simulate these scenarios, four different tool materials with varying heat transfer coefficients were studied (as described in Section 2.2). In addition, for each of the tool grades, six different tool temperatures were simulated (25, 100, 200, 300, 400, 500°C) to investigate the resultant microstructural phases. As the tool temperature increases in a single process cycle even in a water-cooled tool, tool temperatures have been defined as initial conditions rather than boundary conditions in this study.

2.5 PHASE TRANSFORMATION MODEL

The model of predicting the austenite decomposition at arbitrary cooling paths for 22MnB5 steel is based on time-temperature-transformation (TTT) curve and Scheil's additive principle. Using thermal dilation curve in each holding temperature and the metallographic microstructure analysis, the TTT diagram for the 22MnB5 can be obtained, as is shown in Fig.4. The A, F, P, B and M denote austenite, ferrite, pearlite, bainite, and martensite, respectively.

Kinetics [7, 8, 9, and 10] of the diffusional transformation for the isothermal condition can be expressed as the Kinetics [7, 8, 9, and 10] of the diffusional transformation for the isothermal condition can be expressed as the form of JMAK equation:

$$\mathbf{F} = 1 - \exp(-b \times t^n) \qquad (1)$$

If the incubation time of nucleation is considered, the modified form by Hawbolt [11] is expressed as

follows:

$$\mathbf{F} = 1 - \exp[-b(t - t_s)^n] \qquad (3)$$

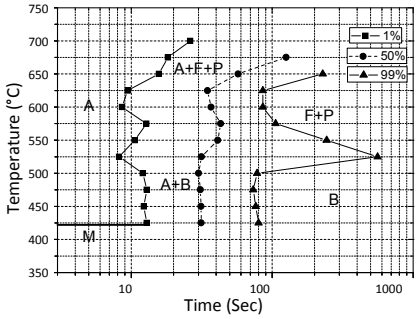

Fig. 4 *The TTT diagram for the 22MnB5*

where F indicates the volume fraction of the phase during the phase transformation, t_s means incubation time of the phase change. Here, b and n are material parameters directly obtained from the TTT diagram.

Scheil's additive rule is adopted to describe the non-isothermal transformation behavior [12]. By this rule, the cooling curve was subdivided into a number of small time steps Δt_i. Then, $\Delta t_i / \tau_i$ is calculated and summed for each time and transformation is assumed to begin when the following equation is fulfilled.

$$\sum_i^m \frac{\Delta t_i}{\tau_i} = 1 \qquad (3)$$

where τ_i is the transformation beginning time at the ith time step.

For the case of the diffusionless transformation, the volume fraction of the martensite is calculated using the empirical model established from experiments by Koistinen and Marburger. The amount of the martensite can be totally expressed as a function of the temperature as follow:

$$\mathbf{F}_m = \{1 - \exp[-0.011(M_s - T)]\} \qquad (3)$$

where $\mathbf{F}_m$ is volume fractions of the martensite. M_s and T are the temperature at which martensite transformation begins and current temperature, respectively. The incubation time has the great influence on the transformation kinetics calculation. It is difficult to measure this value from the dilation curves. So a concise model of incubation time is deduced based on the solution of nonlinear of incubation time on the calculated austenite decomposition kinetics at 600°C. It can be found that both models can predict exactly the transformation JMAK equations system. Fig. 5 shows the effect finishing time. However, the model coupled with the incubation time has the better accuracy on the simulation of transformation kinetics history.

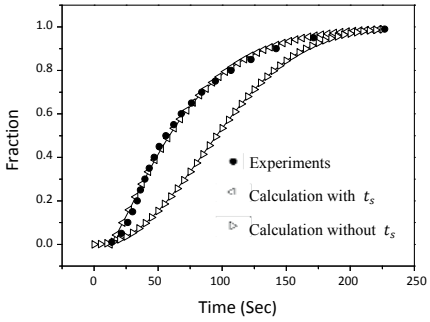

Fig. 5 *The effect of incubation time on the calculation of transformation kinetics*

3 RESULTS AND DISCUSSION

Fig. 6a shows the cooling curves of boron steel sheets where they are cooled down in a tool made of AISI h11 and kept at different temperatures between 25°C and 500°C. The forming process which takes 2 seconds is also included in these cooling curves. The curves belong to a point located in the lower surface of the hat-shaped part. However, the temperature history is identical for all points located in this surface. Tool material AISI h11 with its high conductance leads to very fast cooling rates even by heating it up to high temperatures. As the punch and die clamp the blank, the heat transfer starts rapidly but it slows down as temperature difference between sheet metal and tool becomes smaller. When the tool was heated to 500°C, the minimum cooling rate of 95.4°C/s was achieved. This cooling rate is higher than the critical value 27°C/s and should not normally result phases rather than martensite, but keeping the tool closed for a longer time (approximately 50 seconds) may avoid entering the martensite transformation zone in the CCT diagram and will lead to a bainite transformation in this case.

Fig. 6b to Fig. 6d show the cooling curves achieved for other tool materials including Alumina, Macor and Zirconia respectively. When Alumina was used as the tool material, cooling rates from 21°C/s to 156°C/s were achieved. For Macor, the achievable range of cooling rate is from 5°C/s to 29°C/s. This indicates that a significantly lower tool temperature is needed to reduce the cooling rates below the critical rate when Macor used as the tool material. This will reduce the amount of input energy needed to continuously heat the tool. However, a larger range of cooling rates could be achieved by using Zirconia. Simulations report the range of 14 to 57°C/s when Zirconia used.

These thermo-mechanical simulations were accompanied with a user subroutine that included a modified phase transformation model (as described in Section 2.4), to predict the microstructural phases at the end of quenching process. When the tool temperature is higher than 200°C, the part temperature may not reach the martensite finish temperatu-

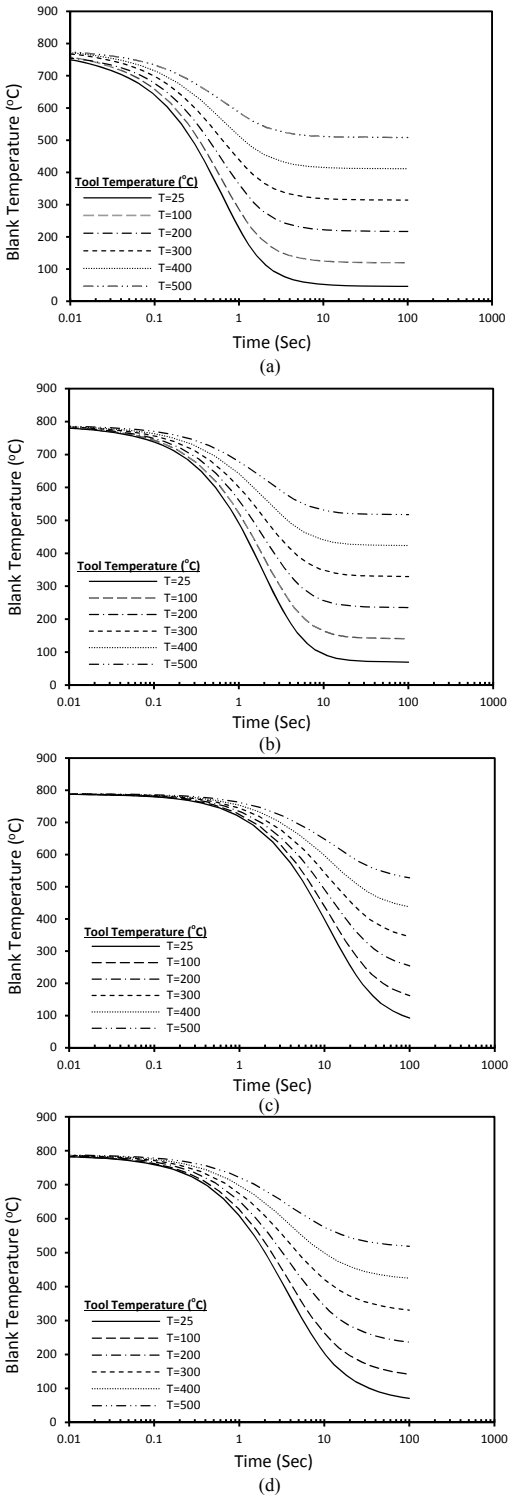

Fig. 6 *Cooling rates of 22MnB5 sheet in (a) AISI h11, (b) Alumina, (c) Macor and (d) Zirconia tool for different tool temperatures*

re (210°C) at the end of the quenching process. Therefore, all the austenitized microstructure will not transform to other phases. The non-transformed fraction of austenite is called retained austenite. A further cooling (e.g. air cooling) may be necessary to cool down the part to the room temperature and complete the transformation.

Fig. 7a shows the resulting martensite fraction for different tool materials and also different temperatures. The phase fractions have been reported for the same point of the part that the cooling curves were reported. For all tool materials, almost all austenite transforms to martensite when the tool temperature is 25°C. As the tool temperature increases, the martensite fraction decreases accordingly. As shown in Fig. 7b, for some specific tool materials and cooling rates, the decrease in martensite fractions is counterbalanced by increased fractions of retained austenite. Moreover, when the tool temperature is 500°C, the fractions of retained austenite are less than 3% for all tool materials. This occurs because the cooling rate is the slowest in this situation and thus, the austenite phase has already transformed to other phases including bainite, ferrite and pearlite in the higher temperatures.

Fig. 7c shows the bainite fractions. The bainite transformation does not occur in AISI h11 tool unless in the tool temperature is higher than 400°C. For the Alumina and Zirconia cases, the tool temperature required for bainite transformation is above 300°C and is less than that for the AISI h11 case. The lowest tool temperature that causes a bainite transformation is approximately 200°C for the Macor tool material case. However, the bainite fraction is just 6% in this situation and can be increased to 35% by increasing the tool temperature up to 300°C.

Fig. 7d shows the accumulated fractions of ferrite and pearlite. These phases require lower cooling rates to appear in comparison with bainite and martensite. As shown, the only situation that will lead to significant fractions of these phases is using Macor tool with high temperature of 500°C. In this situation 18.2% ferrite and 33.3% pearlite transforms.

4 CONCLUSSION

A thermo-mechanical-metallurgical model of hot stamping of boron steel 22MnB5 was created in this study to investigate the effects of tool materials and tool temperatures on consequent microstructural phases of the final product. In this study, most thermo-mechanical parameters were defined in dependency to temperature and would result temperature history with higher accuracy. Moreover, a modified phase transformation model based on Scheil's additive principle has been applied to accurately predict the microstructural phases.

Four different tool materials including AISI h11, Alumina, Macor and Zirconia and a range of 25-500°C for tool temperature have been considered in this new study. Cooling curves related to the quenching process have been achieved and compared together in these situations. The cooling rates in AISI h11 tool were so rapid that the bainite

phase could not appear unless tool temperatures were increased to 500°C.

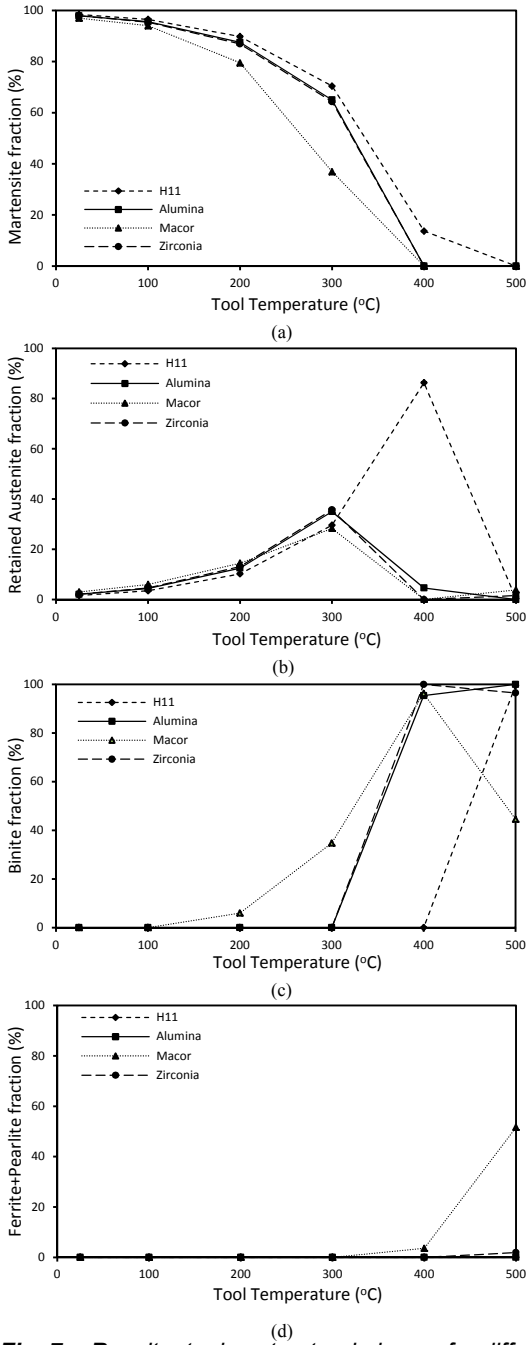

Fig. 7 *Resultant microstructural phases for different tool materials and temperatures*

When using Macor, bainite transformation can occur in lower tool temperature even in 200°C. Moreover, the only configuration that led to significant ferrite and pearlite transformation was using tool made of Macor and heated up to 500°C. This shows that Macor has a strong potential to be utilized in tool design to produce hot stamped parts with tailored mechanical properties. It will result softer phases in the final product and therefore increases ductility and energy absorption.

REFERENCES

[1] George, R., Bardelcik, A., Worswick, M. J.: *Hot forming of boron steels using heated and cooled tooling for tailored properties*. Journal of Materials Processing Technology 212: 2386–2399, 2012.

[2] Picas, I., Hernández, R., Casellas, D., Vails, I.: *Cold cutting of microstructurally tailored hot formed components.* In*:* 2nd International Conf on Hot Sheet Metal Forming of High-Performance Steel, Lulea, Sweden, 115–125, 2009.

[3] Numisheet 2008, *The Numisheet Benchmark Study, Benchmark Problem BM03.* Interlaken, Switzerland, 2008.

[4] Tondini, F., Bosetti, P., Bruschi, S.: *Heat transfer in hot stamping of high-strength steel sheets*. Proc of the Institution of Mechanical Engineers, Part B: Journal of Engineering Manufacture, 225(10): 1813-1824, 2011.

[5] Shapiro, A.B.: *Using LS-Dyna for Hot Stamping.* 7th European LS-Dyna Conf, 2009.

[6] Stoehr, T., Merklein, M., Lechler, J.: *Determination of frictional and thermal characteristics for hot stamping with respect to a numerical process design*. In: 1st International Conf on Hot Sheet Metal Forming of High-Performance Steel, Kassel, Germany, 293-300, 2008.

[7] Johnson, W.A., Mehl, R.F.: *Reaction Kinetion of Nucleation and Growth*. Transaction of AIME, 135: 416-518, 1939.

[8] Avrami, M.: *Kinetics of Phase Change, Part 1: General Theory*, The Journal of Chemical Physics, 7: 1103- 1112, 1939.

[9] Avrami, M.: *Kinetics of Phase Change, Part 2: Transformation Time Relations for Random Distribution of Nuclei*. The Journal of Chemical Physics, 8: 212-224, 1940.

[10] Avrami, M.: *Kinetics of Phase Change, Part 3: Granulation, Phase Change and Microstructure*. The Journal of Chemical Physics, 9: 177-184, 1941.

[11] Hawbolt, E. B., Chau, B., Brimacombe, J. K.: *Kinetics of austenite-pearlite transformation in eutectoid carbon steel.* Metallurgical and Materials Trans A, 14(9): 1803-1815, 1983.

[12] Kwon, H.C., Lee, Y., Kim, S.Y., Woo, J.S., Im, Y.T.: *Numerical prediction of austenite grain size in round-oval-round bar rolling*. ISIJ International, 43: 676–683, 2003.